chloride ions. There is little stacking overlap between adjacent cytosine rings; rather, each ring lies above (and below) the gap between two rings in the neighboring planes. By comparison, in the hydrobromide salt (Bryan & Tomita, 1962) each methylcytosine cation lies above the gap in the center of four rings in the neighboring sheet (Fig. 6).

The close similarity in the intermolecular environments of the two molecules in the asymmetric unit is reflected in their similar patterns of thermal motion (Fig. 1).

We are grateful to Dr Sten Samson for excellent equipment and to Lillian Casler for drawings.

References

BARKER, D. L. & MARSH, R. E. (1964). *Acta Cryst.* **17**, 1581.

BRYAN, R. F. & TOMITA, K. (1962). *Acta Cryst.* **15**, 1174.

BUGG, C. E. & MARSH, R. E. (1976). *J. Mol. Biol.* **25**, 67.

DUCHAMP, D. J. (1964). *Program and Abstracts*, A. C. A. meeting, Bozeman, Montana; paper B-14, p. 29.

International Tables for X-ray Crystallography (1962). Vol. III, Birmingham: Kynoch Press.

JEFFREY, G. A. & KINOSHITA, Y. (1963). *Acta Cryst.* **16**, 20.

JOHNSON, C. K. (1965). *ORTEP*. Report ORNL 3794, Oak Ridge National Laboratory, Oak Ridge, Tennessee.

LARSON, A. C. (1967). *Acta Cryst.* **23**, 664.

STEWART, R. F., DAVIDSON, E. R. & SIMPSON, W. T. (1965). *J. Chem. Phys.* **42**, 3175.

SUNDARALINGAM, M. & JENSEN, L. H. (1965). *J. Mol. Biol.* **13**, 914.

Acta Cryst. (1972). B**28**, 1840

Monoclinic Structure of Synthetic $Ca_5(PO_4)_3Cl$, Chlorapatite

BY P. E. MACKIE, J. C. ELLIOTT* AND R. A. YOUNG

Georgia Institute of Technology, Atlanta, Georgia 30332, *U.S.A.*

(*Received* 27 *April* 1971 *and in revised form* 9 *December* 1971)

Apatites are normally expected to be hexagonal, with space group $P6_3/m$ ($Z=2$), but nearly stoichiometric synthetic chlorapatite is pseudohexagonal, with monoclinic space group $P2_1/b$ ($Z=4$, $a=9{\cdot}628$ (5) Å, $b=2a$, $c=6{\cdot}764$ (5) Å, $\gamma=120°$). The monoclinic and hexagonal structures are very similar, the most significant feature of the monoclinic structure being an ordered arrangement of the Cl atoms above and below $z=\frac{1}{2}$ on the pseudohexagonal axis, such that the mirror plane of the hexagonal structure becomes a glide plane in the monoclinic structure with the doubling of one cell dimension. The mechanism by which the needed ordering information propagates from one Cl column to another involves the occurrence of a Cl atom near the center of one of the two axial triangles of oxygen atoms. The presence of the Cl atom expands the oxygen triangle, thus tilting the associated phosphate tetrahedra and setting off a distortion, propagating *via* ~0·05 Å displacements of columnar Ca ions, which affects the selection of Cl positions in the adjacent unit cells. An active role of Cl vacancies in promoting occurence of the hexagonal phase, and in the apparent development of ferroelectric character in an applied electric field, is suggested. X-ray intensity data from two single-crystal specimens were collected with an automatic diffractometer and led to $R_2(|F|^2) \geq 3{\cdot}4\%$ in least-squares refinements of the structure.

Introduction

By analogy with other apatites that have the space group $P6_3/m$, it has been generally presumed that chlorapatite is hexagonal, with the chlorine ion in the special position at $z=\frac{1}{2}$ (Hendricks, Jefferson & Mosley, 1932). However, nearly stoichiometric synthetic chlorapatite, $Ca_5(PO_4)_3Cl$, exhibits the monoclinic space group $P2_1/b$ (Young & Elliot, 1966). A mineral chlorapatite of nearly stoichiometric chlorine content has also been reported to be similarly monoclinic (Hounslow & Chao, 1970), as have both mineral and synthetic mimetite, $Pb_5(AsO_4)_3Cl$ (Keppler, 1968, 1969). Because monoclinic chlorapatite exhibits almost complete structural similarity to the hexagonal ($P6_3/m$) apatites fluorapatite and hydroxyapatite, the monoclinic cell setting that has the c axis as the unique axis has been chosen to accommodate this similarity. The difference lies primarily in the placement of the halogen ions on columns about 9·6 Å apart. A particular point of interest in the present work is the mechanism by which the ordering information is propagated from column to column, changing the mirror plane of the structure with space group $P6_3/m$ into the glide plane of the structure with space group $P2_1/b$.

The apatite structure has been pictured many times in the literature, most notably by the color overlays in the paper by Beevers & McIntyre (1946). Fig. 1 illustrates the relationship between the unit cell with hexagonal symmetry, generally used for apatites, and the monoclinic unit cell used here. The content of an

* Present address: The London Hospital Medical College, Turner Street, London E.1, England.

hexagonal fluorapatite or hydroxyapatite unit cell can be described in four parts: (1) Ca_I atoms at $z \simeq 0$ and $z \simeq \frac{1}{2}$, forming columns parallel to **c** at $x=\frac{1}{3}$, $y=\frac{2}{3}$ and at $x=\frac{2}{3}$, $y=\frac{1}{3}$; (2) a column of F or OH ions on the screw axis parallel to **c** at $x=0$, $y=0$; (3) two triangular arrays of Ca_{II} atoms on the mirror planes at $z=\frac{1}{4}$ and $z=\frac{3}{4}$ and centered on the screw axis coinciding with the F or OH columns; and (4) six phosphate tetrahedra on the mirror planes. The F ion occurs at $(0,0,\frac{1}{4})$ and $(0,0,\frac{3}{4})$ at the centers of the Ca_{II} triangles, whereas OH is in twofold disorder about the mirror planes, at $0,0,\frac{1}{4}-\Delta$ and $0,0,\frac{1}{4}+\Delta$ ($\Delta \simeq 0{\cdot}19$ for H and 0·05 for O; Sudarsanan & Young, 1969). From a consideration of lattice parameters and normal bond lengths, it was suggested (Young & Elliott, 1966) that the Cl ion, at the same x, y position as F and OH, was displaced from $z=\frac{1}{2}$ by an amount δ, the sign of which was reversed in successive columns as was necessary to accommodate the glide plane which effectively doubled one of the axes perpendicular to the pseudohexagonal axis.

Crystal and X-ray data

The synthetic chlorapatite crystals were grown from solutions of the apatite in fused $CaCl_2$ by Dr J. S. Prener. Chemical analyses reported by him (Prener, 1967), with an error of the order of 0·1 wt.% are 6·72, 38·5, and 54·2 wt.% found for Cl, Ca, and PO_4, respectively, compared with calculated values of 6·81, 38·5 and 54·7. In one case, an additional 1·5% of $Ca_2P_2O_7$ occurred as a separate, probably occluded, phase. The mean refractive index of the crystals, measured with immersion methods, was found to be $1{\cdot}670 \pm 0{\cdot}001$. The birefringence of these crystals has not been fully characterized but is small, its absolute value generally being approximately 0·0002 or less. Mimetic twinning occurred very frequently with the twinned crystals related by a 120° rotation about the *c* axis (pseudohexagonal axis). Nevertheless, it was possible for an untwinned single-crystal specimen to be selected for the X-ray diffraction measurements. The X-ray reflection

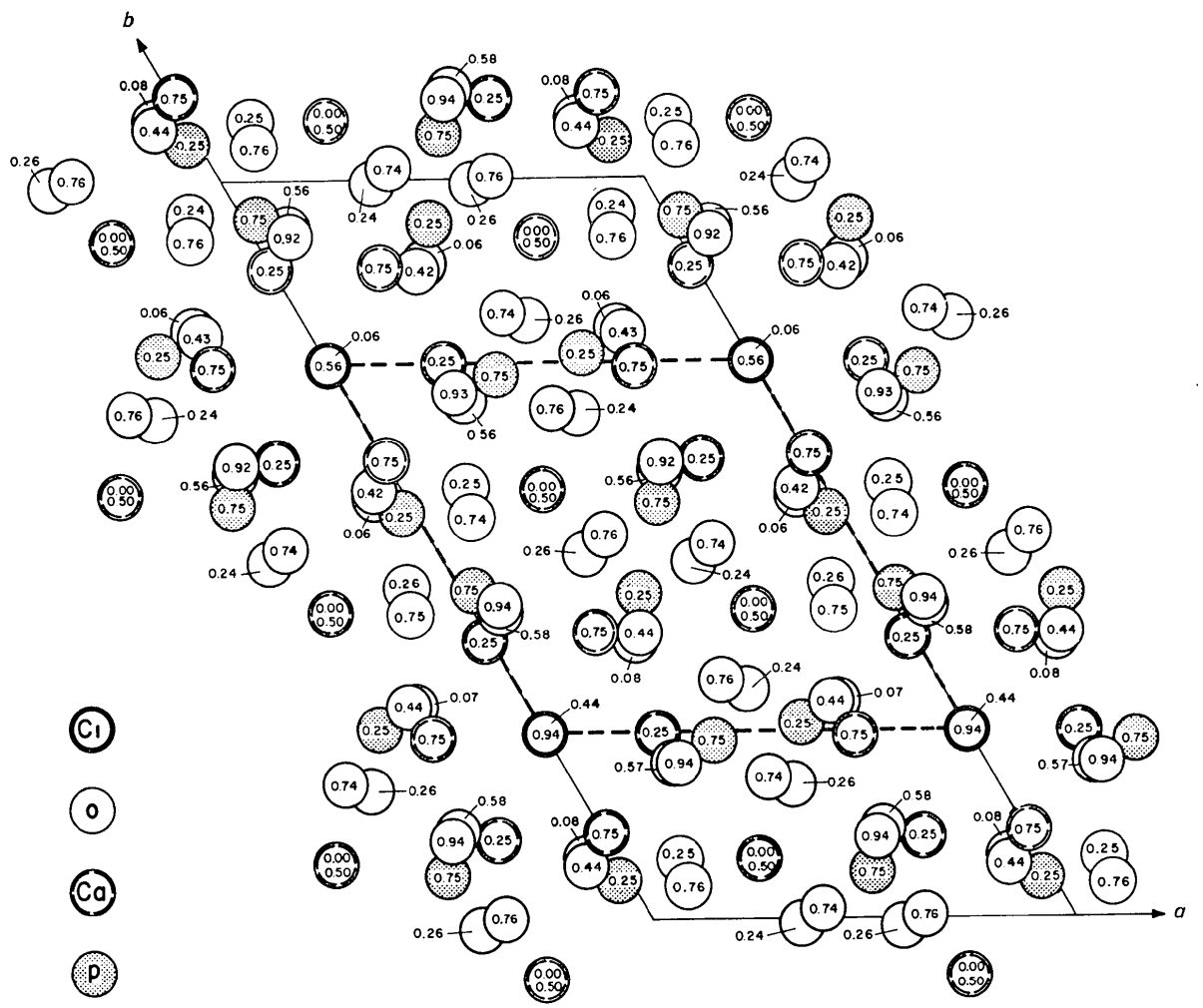

Fig. 1. Projection of the x,y plane of the chlorapatite structure, showing relation between the monoclinic unit cell chosen and the hexagonal unit cell used for fluor- and hydroxyapatite.

Table 1. *Structure amplitudes and errors for monoclinic 'chlorapatite'*

$|F|^2_{cal}$ is based on model with Cl site of second kind unoccupied; extinction corrections have been applied to $|F|_{obs}$. $|F_{000}| = 1032$.

intensity data were collected with a punched-tape-controlled automatic single-crystal diffractometer, employing Mo $K\alpha$ radiation ($\lambda = 0{\cdot}70926$ Å). Further details are given in the Appendix.

Least-squares refinements

It has been noted previously (Prener, 1967; Young & Elliott, 1966) that loss of, or substitution for, only a small fraction of the Cl ions changes the symmetry to hexagonal. Prener (1967) also has shown by X-ray and optical means that a reversible transition to the hexagonal phase takes place at about 200 °C. These observations, plus the facts that $b = 2a$ and $\gamma = 120°$, all attest to the strongly pseudohexagonal character of the monoclinic form at room temperature. In fact, seemingly good least-squares refinements could be obtained in the hexagonal space group if one used anisotropic temperature factors and simulated the effect of the glide plane with twofold disorder of the chlorine ions, only, about the mirror plane. Such a least-squares refinement in $P6_3/m$, based on 441 reflec-

Table 2. *Atom parameters derived from least-squares refinements in two space groups*

Atom Parameters (1)	$P6_3/m$ (2)	$P2_1/b$ (3)		
ATOM	O_I	O_{Ia}	O_{Ib}	O_{Ic}
X	34366	34361 [34368]	49241 [49295]	14851 [14946]
Y	49285	49601 [49643]	32401 [32466]	57831 [57825]
Z	1/4	23633 [1/4]	75543 [3/4]	24803 [1/4]
β_{11}	45740	53314 [45740]	39033 [41903]	16311 [1348]
β_{22}	41940	1067 [1053]	356 [342]	1346 [1141]
β_{33}	50253	40423 [50253]	42922 [5025]	40813 [5025]
β_{12}	37136	1846 [1886]	35 [242]	705 [435]
β_{13}	0	-5925 [0]	-819 [0]	-2717 [0]
β_{23}	0	-913 [0]	-713 [0]	-514 [0]
MULTIPLIER	1/2	1.01715 [1]	1.0089 [1]	1.0189 [1]
ATOM	O_{II}	O_{IIa}	O_{IIb}	O_{IIc}
X	59274	59241 [5927.]	53421 [$5343$5]	12701 [12709]
Y	46585	48271 [$4829$2]	31381 [$3135$5]	54621 [5464.]
Z	1/4	23903 [1/4]	24473 [1/4]	73663 [3/4]
β_{11}	153_{28}	156_{11} [153_{28}]	247_{12} [242_{31}]	276_{12} [$277$9]
β_{22}	242_{31}	676 [618]	827 [692]	526 [387]
β_{33}	773_{65}	581_{30} [773_{65}]	637_{25} [773_{65}]	570_{34} [773_{65}]
β_{12}	59_{26}	345 [30_{13}]	805 [923]	535 [473]
β_{13}	0	73_{16} [0]	-32_{19} [0]	53_{16} [0]
β_{23}	0	611 [0]	-18_{13} [0]	4411 [0]
MULTIPLIER	1/2	0.9939 [1]	1.0129 [1]	0.997_{10} [1]
ATOM	O_{III}	O_{IIIa}	O_{IIIb}	O_{IIIc}
X	35424	34112 [3541.]	73602 [$7324$3]	8262 [$866$7]
Y	26773	38041 [$3838$2]	29181 [$2933$9]	42041 [$4271$1]
Z	6715	7693 [$670$5]	7233 [$670$5]	57743 [$5670$5]
β_{11}	713_{33}	684_{21} [713_{33}]	337_{17} [391_{22}]	405_{17} [$388$2]
β_{22}	391_{22}	102_{8} [$98$5]	83_{8} [$97$2]	147_{9} [$178$8]
β_{33}	530_{39}	429_{39} [530_{39}]	503_{43} [530_{39}]	409_{36} [530_{39}]
β_{12}	358_{23}	154_{8} [179_{11}]	29_{7} [$17$0]	168_{8} [$178$5]
β_{13}	-411_{38}	-322_{25} [-411_{38}]	199_{18} [310_{18}]	-130_{17} [-101_{3}]
β_{23}	-310_{35}	-95_{12} [-155_{18}]	-41_{13} [$-51$2]	-133_{13} [-206_{19}]
MULTIPLIER	1	1.014_{11} [1]	0.992_{11} [1]	0.99_{111} [1]
ATOM		O'_{IIIa}	O'_{IIIb}	O'_{IIIc}
X		3645_{2} [3541_{4}]	7300_{2} [7324_{3}]	894_{1} [866_{7}]
Y		3866_{1} [3838_{2}]	2950_{1} [2933_{2}]	4327_{1} [4271_{1}]
Z		4413_{3} [4330_{5}]	4371_{3} [4330_{5}]	9419_{3} [9330_{5}]
β_{11}		411_{16} [713_{33}]	345_{17} [391_{22}]	269_{15} [388_{2}]
β_{22}		100_{8} [98_{5}]	72_{8} [97_{2}]	110_{8} [178_{8}]
β_{33}		366_{30} [530_{39}]	312_{35} [530_{39}]	344_{29} [530_{39}]
β_{12}		123_{7} [179_{11}]	30_{7} [17_{0}]	88_{7} [178_{5}]
β_{13}		147_{16} [411_{38}]	-174_{17} [-310_{35}]	24_{15} [101_{3}]
β_{23}		74_{12} [155_{18}]	40_{13} [51_{1}]	104_{12} [206_{11}]
MULTIPLIER		0.997_{0} [1]	0.972_{13} [1]	0.990_{10} [1]

Atom Parameters (1)	$P6_3/m$ (2)	$P2_1/b$ (3)		
ATOM	Ca_I	Ca_I	Ca_I'	
X	1/3	3276_{1} [1/3]	3387_{1} [1/3]	
Y	2/3	5811_{2} [7/12]	5856_{0} [7/12]	
Z	38_{2}	34_{1} [38_{2}]	4966_{1} [4962_{1}]	
β_{11}	316_{1}	263_{5} [316_{6}]	251_{6} [316_{6}]	
β_{22}	316_{1}	79_{3} [79_{2}]	79_{3} [79_{2}]	
β_{33}	210_{1}	194_{8} [210_{11}]	266_{6} [210_{11}]	
β_{12}	158_{1}	61_{2} [79_{2}]	69_{2} [79_{2}]	
β_{13}	0	0_{3} [0]	-2_{3} [0]	
β_{23}	0	-6_{2} [0]	-2_{2} [0]	
MULTIPLIER	1/3	0.959_{4} [1]	0.953_{4} [1]	
ATOM	Ca_{II}	Ca_{IIa}	Ca_{IIb}	Ca_{IIc}
X	2596_{1}	2594_{2} [2596_{2}]	53_{0} [52_{1}]	2550_{2} [2544_{2}]
Y	52_{1}	2523_{2} [2526_{2}]	6229_{1} [6228_{1}]	3798_{0} [3798_{1}]
Z	1/4	2480_{1} [1/4]	7481_{1} [3/4]	7513_{1} [3/4]
β_{11}	239_{2}	230_{3} [239_{8}]	280_{3} [272_{8}]	273_{3} [272_{7}]
β_{22}	273_{2}	74_{2} [68_{2}]	71_{2} [68_{3}]	59_{2} [69_{2}]
β_{33}	293_{2}	256_{4} [293_{12}]	267_{4} [293_{12}]	256_{5} [293_{1}]
β_{12}	120_{1}	62_{2} [60_{4}]	81_{2} [77_{2}]	54_{2} [60_{2}]
β_{13}	0	27_{3} [0]	6_{2} [0]	17_{3} [0]
β_{23}	0	1_{3} [0]	19_{3} [0]	10_{3} [0]
MULTIPLIER	1/2	0.962_{3} [1]	0.965_{2} [1]	0.962_{3} [1]
ATOM	P	P_a	P_b	P_c
X	4078_{1}	4076_{2} [4078_{1}]	6259_{0} [6246_{1}]	3245 [3243]
Y	3756_{1}	4376_{2} [4377_{1}]	2665_{1} [2662_{1}]	4538_{0} [4539_{1}]
Z	1/4	2533_{1} [1/4]	2522_{1} [1/4]	7517_{1} [3/4]
β_{11}	163_{9}	182_{4} [163_{5}]	163_{4} [159_{5}]	151_{4} [136_{5}]
β_{22}	159_{10}	43_{2} [40_{1}]	40_{2} [34_{1}]	50_{2} [41_{1}]
β_{33}	235_{15}	221_{6} [235_{15}]	215_{6} [235_{15}]	227_{6} [235_{15}]
β_{12}	93_{8}	48_{2} [46_{4}]	32_{2} [33_{2}]	42_{2} [35_{1}]
β_{13}	0	-10_{6} [0]	4_{6} [0]	-10_{6} [0]
β_{23}	0	-3_{4} [0]	-4_{4} [0]	-6_{4} [0]
MULTIPLIER	1/2	1.027_{3} [1]	1.024_{3} [1]	1.027_{3} [1]
ATOM	Cl	Cl	Cl'	
X	0	16_{1} [0]	34_{6} [0]	
Y	0	2493_{1} [1/4]	2483_{2} [1/4]	
Z	4438_{6}	4439_{2} [4438_{6}]	5758_{6} [5562_{6}]	
β_{11}	339_{1}	287_{5} [339_{1}]	167_{8} [339_{1}]	
β_{22}	339_{1}	74_{2} [85_{2}]	31_{39} [85_{2}]	
β_{33}	955_{5}	914_{12} [955_{5}]	999_{1179} [955_{5}]	
β_{12}	170_{1}	71_{2} [85_{5}]	3_{121} [85_{5}]	
β_{13}	0	12_{7} [0]	5_{337} [0]	
β_{23}	0	-9_{6} [0]	-68_{355} [0]	
MULTIPLIER	1/6	0.931_{4} [1-M(Cl')]	0.021_{4} [1-M(Cl)]	

NOTES:

(1) All positional parameters, except those written as fractions, have been multiplied by 10^4. All temperature parameters have been multiplied by 10^5. Standard deviations are shown as subscripts.

(2) This column gives the results in $P6_3/m$ with the Cl assumed to be in two-fold disorder about the mirror plane.

(3) Enclosed in brackets after the results obtained in $P2_1/b$ are the parameters obtained in $P6_3/m$ transformed to the equivalent position in the monoclinic cell. The origin of the monoclinic cell was taken at (0, -¼, 0) of the hexagonal cell.

tions from a 0·18 mm diameter spherical specimen, yielded $R_2=5{\cdot}5\%$ and $wR_2=11{\cdot}3\%$ with 40 parameters varied.

$$\text{Here, } R_2=\frac{\sum||F_o|^2-|F_c|^2|}{\sum|F_o|^2}$$

$$\text{and } wR_2=\frac{[\sum w(|F_o|^2-|F_c|^2)^2]^{1/2}}{[\sum w|F_o|^4]^{1/2}}, \text{ where}$$

w is the reciprocal of the variance for each observation and the summation is carried out over all observations. (The results are included in Table 2, under the heading '$P6_3/m$', to permit comparisons with the true structural parameters.)

The final refinements in $P2_1/b$ were based on 2232 reflections, of which 976 could occur only in the monoclinic space group, collected from a 0·31 mm diameter spherical specimen. After extinction corrections (Zachariasen, 1963) had been made, a full-matrix least-squares adjustment using both real and imaginary parts of the dispersion corrections (Cromer, 1965) gave $R_2=2{\cdot}5\%$ and $wR_2=3{\cdot}5\%$. The relevant structure-factor values are listed in Table 1.

During the final cycles of the refinement, the overall scale factor was fixed and the site occupancy factors (multipliers) for the atoms were allowed to vary with no constraint imposed to maintain charge balance. These unconstrained refinements led to a charge imbalance of $-0{\cdot}273\pm0{\cdot}3$ electrons per asymmetric unit containing, if stoichiometric, 258 electrons.

Results

The unit cell of monoclinic chlorapatite contains four formula units of $Ca_5(PO_4)_3Cl$ with all of the atoms in general positions. The final positional and thermal parameters are listed in Table 2 in such a way as to permit easy identification of the departures of the parameters from the values they would have if the crystal were hexagonal rather than monoclinic. As anticipated, the principal distinguishing feature of the monoclinic structure is the position of the chlorine ion. Note that the z coordinates of the chlorine atoms in the two cases (refined in $P6_3/m$ and in $P2_1/b$) agree within 0·001 Å, while their positions in the x, y plane, although similar, differ significantly. In the monoclinic structure, the chlorine is displaced ~0·02 Å from the screw axis, and the columnar calcium ions, Ca_I are displaced ~0·05 Å from their threefold axis positions in the hexagonal structure.

The environment of the chlorine ions is shown in Fig. 2. The chlorine atom is 0·38 Å, or about 6% of the length of the c axis, distant from the position previously assumed for it midway between Ca triangles (at $0,\frac{1}{4},\frac{1}{2}$ in the monoclinic cell); also, it occurs in the ordered arrangement consistent with the glide plane. This position yields a Ca–Cl bond length of 2·80 Å, in reasonable agreement with the 2·73 Å bond distance quoted by Sutton (1958) and in contradistinction to a 3·01 Å bond distance that would occur if chlorine were at $z=\frac{1}{2}$.

Prener (1967) has commented on the tendency of these flux-grown crystals to be Cl-deficient and has shown (Prener, 1971) that the deficiency occurs by loss of $CaCl_2$ with consequent changes in lattice parameters. By comparison with Prener's values, our lattice parameters suggest a Cl deficiency of 3 to 5%. The atomic multipliers in Table 2 corroborate such a Cl deficiency, indicating that only about 95% of the stoichiometric amount of Cl is present. The atomic multipliers for Ca suggest that there is also a deficiency of Ca, at least sufficient to affirm the loss of $CaCl_2$.

Such implied Cl vacancies would remove the steric restraint, otherwise imposed by Cl–Cl contact, on strict ordering within a Cl-ion column. This would permit individual or groups of Cl ions within a given column to occur, for example, at or near $z=0{\cdot}06$ and 0·56 rather than at 0·44 and 0·94. In fact, the rather short Cl–Cl distance along the column (3·38 *vs.* 3·92 Å for the sum of ionic radii) would seem to pro-

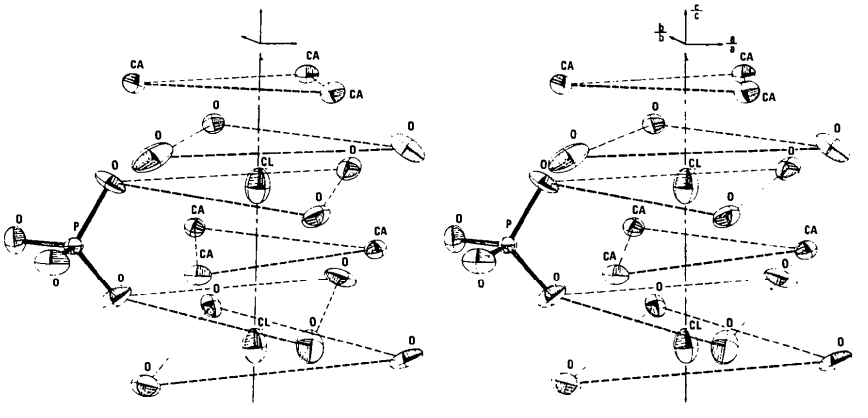

Fig. 2. Stereographic view of environment of the chlorine ions. The ellipsoids represent r.m.s. thermal vibrational amplitudes, not ion sizes. The stereographic plot was made with Johnson's (1965) *ORTEP* program. Unit vectors along the axial directions are shown as, for example, **b**/*b*, *etc.*

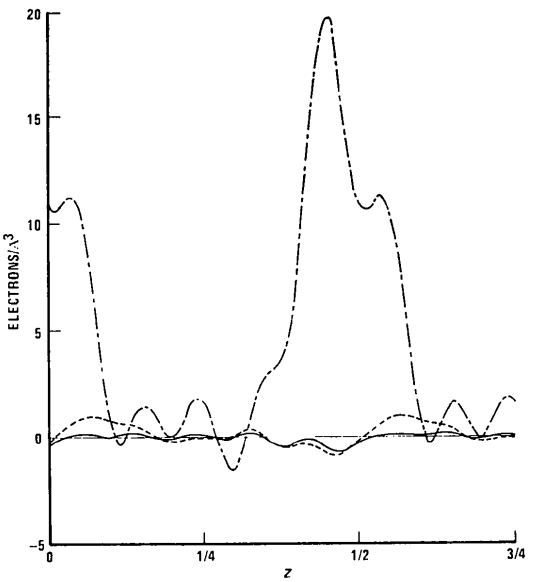

Fig. 3. Electron density difference syntheses along the screw axis with (*a*) no Cl ions in model denoted by –·–·–· (*b*) 0·93 Cl at 0, ¼, 0·444 denoted by -------. (*c*) 0·93 Cl at 0, ¼, 0·444 and 0·02 Cl′ at 0, ¼, 0·576 denoted by ———.

mote such displacements of individual Cl ions adjacent to Cl vacancies. On the basis of least-squares analyses of single-crystal X-ray data, Hounslow (1968) and Hounslow & Chao (1970) have reported such disordering in a monoclinic mineral chlorapatite, which is also somewhat Cl deficient. Hence, least-squares refinements and difference maps were employed to assess the possibility that, although most of the Cl ions occur at the $z=0{\cdot}44$ and 0·94 sites, some might be present at $z=0{\cdot}06$ and 0·56 sites in the same columns. Least-squares adjustments of all variable parameters led to $wR_2=3{\cdot}53\%$ with Cl at only the first sites. With Cl also permitted at the second sites (refined values $z=0{\cdot}08$ and 0·58), $wR_2=3{\cdot}35\%$ was obtained and the site occupancy factor did not fall below approximately 2% (see Cl′ in Table 2). A difference synthesis relating to this point, and leading to a similar conclusion that approximately 2% of the Cl sites of the second kind are filled, is shown in Fig. 3.

It seems most probable that this small amount of Cl occurs at the second site because of vacancy-induced disordering, as discussed above. It seems improbable that the apparent occupancy of the second Cl site is due to a small amount of twinning, as the extra reflections associated with it were not observed either with the diffractometer or with long-exposure photographs (precession and Weissenberg).

Table 3 lists some of the bond distances and angles. The PO_4 tetrahedra are significantly distorted, being elongated along the $P–O_{II}$ direction. This direction lies essentially in the glide plane. The various dihedral angles within a given tetrahedron differ by as much as 6°, which is $> 50\sigma$. In fluorapatite and hydroxyapatite, the PO_4 tetrahedra show this same type of distortion to a very similar degree (Young, Sudarsanan & Mackie, 1968).

Statistically significant differences exist among the three crystallographically distinct PO_4 tetrahedra in this monoclinic chlorapatite (Table 3). Thus, present results support Prener's (1967) expectation of real differences among the phosphate tetrahedra in chlorapatite, on the basis of which he was able to account for the threefold splitting of a fluorescence emission line at about 8600 cm^{-1} in crystals doped with MnO_4^{-3}. Similarly doped fluorapatite did not show such splitting.

Discussion: mechanism of ordering

The development of a monoclinic structure from the ordering of the Cl displacements requires both ordering within a column and ordering between columns. The ordering within a column is easily understood in terms of the rather short Cl–Cl distance of 3·38 Å (compared with 3·87 Å in $CaCl_2$). The question then remains as to how the glide plane is enforced. As is shown by Table 2, the other atoms are displaced rather little from the positions they would occupy in $P6_3/m$. Although the displacement of the chlorine from the ideal symmetry position permits formation of electric dipoles, it is probably not reasonable to expect direct dipole–dipole coupling, over a distance of 9·6 Å through many intervening atoms, to be the mechanism of ordering between columns. Instead of such a mechanism, then, one looks for a steric reason, such as a rumpling in the structure, involving displacements from the mirror-plane positions of the hexagonal structure, twisting of the tetrahedra, *etc.*

The three oxygen atoms nearest the chlorine atom (Fig. 2) have very nearly the same *z* coordinate as that of the chlorine and thus one might regard the chlorine as being approximately in the center of a triangle of O'_{III} atoms in which the chlorine–oxygen distances are 3·15 Å. From Table 3, we see that the perimeter of the O'_{III} triangle, which contains a chlorine ion, is nearly 0·9 Å larger than that of the O_{III} triangle, which does not contain a chlorine ion (Fig. 1). In Fig. 2, one sees that enlargement of the chlorine-containing O'_{III} triangle tilts the associated PO_4 groups. This tilt carries the ordering information nearly halfway to the next chlorine-ion column. We then require to understand (1) how the ordering information is passed on to the next set of phosphate tetrahedra (attached to the O_{III} triangle surrounding the next chlorine-ion column) and (2) how the information is now passed differently along the three hexagonal *a*-axis directions so that they are no longer equivalent, the overall symmetry is lowered, and the glide-plane ordering can occur. The answer to both questions appears to lie in the shift of the position of the Ca_I ion (Table 2). In the hexagonal cell, these ions are on a threefold axis. In the monoclinic cell, they are not. The two Ca_I ions at $\frac{1}{3},\frac{2}{3},z$ and $\frac{1}{3},\frac{2}{3},\frac{1}{2}-z$ in the hexagonal cell are shifted in

the monoclinic cell by about 0.05 Å in opposite directions. The sense of these Ca_I shifts is then communicated to the coordinating PO_4 groups, and their responding small changes, in turn, impose the preferred choice of chlorine position (*e.g.* $z = 0{\cdot}56$ *vs.* 0·44) in the next column. In Fig. 1, *all* of the Ca_I shifts are approximately along the [11.0] direction. Such shifts are commensurate with 2_1 symmetry, but not with 6_3 symmetry. Thus, the ordering information is propagated differently along the three directions that

Table 3. *Interatomic angles and distances in synthetic monoclinic 'chlorapatite'*

a. IN PO_4 TETRAHEDRA

Atoms*	Angle** (degrees)	Atoms*	Interatomic** distance (Å)
$O_{Ia(0,0)}$ - $P_{a(0,0)}$ - $O_{IIa(0,0)}$	111.33 (8)	$P_{a(0,0)}$ - $O_{Ia(0,0)}$	1.529 (2)
$O_{Ia(0,0)}$ - $P_{a(0,0)}$ - $O_{IIIa(0,0)}$	111.23 (10)	$P_{a(0,0)}$ - $O_{IIa(0,0)}$	1.544 (1)
$O_{Ia(0,0)}$ - $P_{a(0,0)}$ - $O'_{IIIa(0,0)}$	112.34 (10)	$P_{a(0,0)}$ - $O_{IIIa(0,0)}$	1.530 (2)
$O_{IIa(0,0)}$ - $P_{a(0,0)}$ - $O_{IIIa(0,0)}$	107.76 (10)	$P_{a(0,0)}$ - $O'_{IIIa(0,0)}$	1.532 (2)
$O_{IIa(0,0)}$ - $P_{a(0,0)}$ - $O'_{IIIa(0,0)}$	106.22 (9)		
$O_{IIIa(0,0)}$ - $P_{a(0,0)}$ - $O'_{IIIa(0,0)}$	107.70 (10)		
$O_{Ib(2,2)}$ - $P_{b(4,3)}$ - $O_{IIb(4,3)}$	111.21 (8)	$P_{b(4,3)}$ - $O_{Ib(2,2)}$	1.531 (2)
$O_{Ib(2,2)}$ - $P_{b(4,3)}$ - $O_{IIIb(4,3)}$	111.88 (10)	$P_{b(0,0)}$ - $O_{IIb(0,0)}$	1.544 (2)
$O_{Ib(2,2)}$ - $P_{b(4,3)}$ - $O'_{IIIb(4,3)}$	112.07 (10)	$P_{b(0,0)}$ - $O_{IIIb(0,0)}$	1.532 (2)
$O_{IIb(0,0)}$ - $P_{b(0,0)}$ - $O_{IIIb(0,0)}$	107.30 (11)	$P_{b(0,0)}$ - $O'_{IIIb(0,0)}$	1.529 (2)
$O_{IIIb(0,0)}$ - $P_{b(0,0)}$ - $O'_{IIIb(0,0)}$	106.51 (11)		
$O_{IIIb(0,0)}$ - $P_{b(0,0)}$ - $O'_{IIIb(0,0)}$	107.58 (8)		
$O_{Ic(0,3)}$ - $P_{c(3,0)}$ - $O_{IIc(3,0)}$	111.25 (8)	$P_{c(3,0)}$ - $O_{Ic(0,3)}$	1.529 (2)
$O_{Ic(0,3)}$ - $P_{c(3,0)}$ - $O_{IIIc(3,0)}$	111.49 (9)	$P_{c(0,0)}$ - $O_{IIc(0,0)}$	1.545 (2)
$O_{Ic(0,3)}$ - $P_{c(3,0)}$ - $O'_{IIIc(3,0)}$	112.23 (10)	$P_{c(0,0)}$ - $O'_{IIIc(0,0)}$	1.532 (2)
$O_{IIc(0,0)}$ - $P_{c(0,0)}$ - $O_{IIIc(0,0)}$	107.70 (10)	$P_{c(0,0)}$ - $O_{IIIc(0,0)}$	1.532 (2)
$O_{IIc(0,0)}$ - $P_{c(0,0)}$ - $O'_{IIIc(0,0)}$	106.11 (10)		
$O'_{IIIc(0,0)}$ - $P_{c(0,0)}$ - $O_{IIIc(0,0)}$	107.79 (10)		

b. IN OXYGEN TRIANGLES

Oxygen Triangle with Cl at Center

Atoms*	Interatomic** distance (Å)	Atoms*	Angle** (degrees)
$O'_{IIIa(0,0)}$ - $O'_{IIIb(1,0)}$	5.446 (4)	$O'_{IIIa(0,0)}$ - $O'_{IIIb(0,0)}$ - $O'_{IIIc(2,1)}$	60.30 (4)
$O'_{IIIa(0,0)}$ - $O'_{IIIc(2,1)}$	5.480 (4)	$O'_{IIIa(0,0)}$ - $O'_{IIIc(2,1)}$ - $O'_{IIIb(1,0)}$	59.67 (4)
$O'_{IIIc(2,1)}$ - $O'_{IIIb(1,0)}$	5.466 (4)	$O'_{IIIb(1,0)}$ - $O'_{IIIa(0,0)}$ - $O'_{IIIc(2,1)}$	60.03 (4)

Greatest difference in z coordinates = 0.005 Å; Greatest difference in side lengths = 0.034 (6) Å;
Perimeter = 16.392 (7) Å

Oxygen Triangle without Cl at Center

Atoms*	Interatomic** distance (Å)	Atoms*	Angle** (degrees)
$O_{IIIa'(0,0)}$ - $O_{IIIb(1,0)}$	5.189 (4)	$O_{IIIc(2,1)}$ - $O_{IIIb(1,0)}$ - $O_{IIIa'(0,0)}$	59.59 (4)
$O_{IIIa'(0,0)}$ - $O_{IIIc(2,1)}$	5.154 (4)	$O_{IIIc(2,1)}$ - $O_{IIIa'(0,0)}$ - $O_{IIIb(1,0)}$	60.23 (4)
$O_{IIIb(1,0)}$ - $O_{IIIc(2,1)}$	5.185 (4)	$O_{IIIa'(0,0)}$ - $O_{IIIc(2,1)}$ - $O_{IIIb(1,0)}$	60.18 (4)

Greatest difference in z coordinates = 0.005 Å; Greatest difference in side lengths = 0.035 (6) Å;
Perimeter = 15.528 (7) Å

c. O-O INTERATOMIC DISTANCES

Atoms*	Interatomic** Distance (Å)
$O_{Ia(0,0)}$ - $O_{IIa(0,0)}$	2.537 (2)
$O_{Ia(0,0)}$ - $O_{IIIa(0,0)}$	2.524 (3)
$O_{Ia(0,0)}$ - $O_{III'a(0,0)}$	2.543 (3)
$O_{IIa(0,0)}$ - $O_{IIIa(0,0)}$	2.483 (2)
$O_{IIa(0,0)}$ - $O_{III'a(0,0)}$	2.460 (2)
$O_{IIIa(0,0)}$ - $O_{III'a(0,0)}$	2.473 (3)
$O_{Ib(7,1)}$ - $O_{IIb(0,0)}$	2.538 (3)
$O_{Ib(7,1)}$ - $O_{IIIb(0,0)}$	2.537 (2)
$O_{Ib(7,1)}$ - $O_{III'b(0,0)}$	2.538 (2)
$O_{IIb(0,0)}$ - $O_{IIIb(0,0)}$	2.477 (2)
$O_{IIb(0,0)}$ - $O_{III'b(0,0)}$	2.463 (2)
$O_{IIIb(0,0)}$ - $O_{III'b(0,0)}$	2.470 (3)
$O_{Ic(3,3)}$ - $O_{IIc(0,0)}$	2.537 (2)
$O_{Ic(3,3)}$ - $O_{IIIc(0,0)}$	2.530 (2)
$O_{Ic(3,3)}$ - $O_{III'c(0,0)}$	2.541 (2)
$O_{IIc(0,0)}$ - $O_{IIIc(0,0)}$	2.484 (3)
$O_{IIc(0,0)}$ - $O_{III'c(0,0)}$	2.459 (3)
$O_{IIIc(0,0)}$ - $O_{III'c(0,0)}$	2.476 (3)

d. Ca_{II}-O INTERATOMIC DISTANCES

Atoms*	Interatomic** Distance (Å)
$Ca_{IIa(0,0)}$ - $O_{Ic(6,2)}$	2.964 (2)
$Ca_{IIb(3,3)}$ - $O_{Ia(0,0)}$	2.973 (2)
$Ca_{IIc(0,0)}$ - $O_{Ib(0,0)}$	2.973 (2)
$Ca_{IIa(0,0)}$ - $O_{IIb(0,0)}$	2.295 (2)
$Ca_{IIb(3,3)}$ - $O_{IIc(3,3)}$	2.301 (2)
$Ca_{IIc(0,0)}$ - $O_{IIa(4,3)}$	2.299 (2)
$Ca_{IIa(0,0)}$ - $O_{IIIa(0,0)}$	2.471 (2)
$Ca_{IIb(3,3)}$ - $O_{IIIb(1,0)}$	2.507 (2)
$Ca_{IIc(0,0)}$ - $O_{IIIc(0,0)}$	2.460 (2)
$Ca_{IIa(0,0)}$ - $O'_{IIIa(0,0)}$	2.609 (2)
$Ca_{IIb(3,3)}$ - $O'_{IIIb(1,0)}$	2.557 (2)
$Ca_{IIc(0,0)}$ - $O'_{IIIc(0,0)}$	2.621 (2)
$Ca_{IIa(0,0)}$ - $O_{IIIb(1,1)}$	2.361 (3)
$Ca_{IIb(3,3)}$ - $O_{IIIc(0,0)}$	2.357 (3)
$Ca_{IIc(0,0)}$ - $O_{IIIa(8,0)}$	2.351 (3)
$Ca_{IIa(0,0)}$ - $O'_{IIIb(7,1)}$	2.314 (3)
$Ca_{IIb(3,3)}$ - $O'_{IIIc(2,0)}$	2.323 (3)
$Ca_{IIc(0,0)}$ - $O'_{IIIa(0,0)}$	2.321 (3)

e. Ca_I-O INTERATOMIC DISTANCES

Atoms*	Interatomic** Distance (Å)
$Ca_{I(0,0)}$ - $O_{Ia(0,0)}$	2.427 (2)
$Ca_{I(0,0)}$ - $O_{Ib(4,3)}$	2.416 (2)
$Ca_{I(0,0)}$ - $O_{Ic(0,0)}$	2.370 (2)
$Ca_{I(0,0)}$ - $O_{IIa(5,3)}$	2.395 (2)
$Ca_{I(0,0)}$ - $O_{IIb(5,3)}$	2.447 (2)
$Ca_{I(0,0)}$ - $O_{IIc(2,0)}$	2.477 (2)
$Ca'_{I(0,0)}$ - $O_{IIa(4,3)}$	2.498 (2)
$Ca'_{I(0,0)}$ - $O_{IIb(4,3)}$	2.438 (2)
$Ca'_{I(0,0)}$ - $O_{IIc(0,0)}$	2.413 (2)
$Ca'_{I(0,0)}$ - $O_{Ia(0,0)}$	2.388 (2)
$Ca'_{I(0,0)}$ - $O_{Ib(4,3)}$	2.397 (2)
$Ca'_{I(0,0)}$ - $O_{Ic(0,0)}$	2.438 (2)
$Ca_{I(8,0)}$ - $O_{IIIa(4,3)}$	2.942 (2)
$Ca_{I(8,0)}$ - $O_{IIIb(4,3)}$	2.850 (2)
$Ca_{I(8,0)}$ - $O_{III'c(0,0)}$	2.655 (2)
$Ca_{I'(0,0)}$ - $O_{III'a(4,3)}$	2.665 (2)
$Ca_{I'(0,0)}$ - $O_{III'b(4,3)}$	2.729 (2)
$Ca_{I'(0,0)}$ - $O_{IIIc(0,0)}$	2.941 (2)

f. Ca_{II}-Cl INTERATOMIC DISTANCES

Atoms*	Interatomic** Distance (Å)
Cl - $Ca_{IIa(0,0)}$	2.789 (1)
Cl - $Ca_{IIb(3,3)}$	2.811 (2)
Cl - $Ca_{IIc(2,1)}$	2.800 (1)

g. O_{III}-Cl INTERATOMIC DISTANCES

Atoms*	Interatomic** Distance (Å)
Cl - $O'_{IIIa(0,0)}$	3.156 (2)
Cl - $O'_{IIIb(1,0)}$	3.148 (2)
Cl - $O'_{IIIc(2,1)}$	3.159 (2)

*$ATOM_{(i,j)}$ is $ATOM_{(0,0)}$ after cell translation i and symmetry operation j have been performed.

i	x'	y'	z'
0	x	y	z
1	x-1	y	z
2	x	y	z-1
3	x	y-1	z-1
4	x-1	y-1	z-1
5	x-1	y-1	z
6	x	y-1	z
7	x-1	y	z-1
8	x	y	z+1

j	x''	y''	z''
0	x	y	z
1	$\bar{x}$'	1/2+y'	1/2+z'
2	x'	1/2+y'	1/2-z'
3	$\bar{x}$'	$\bar{y}$'	$\bar{z}$'

**The cell parameters and associated errors used in the interatomic distance and angle calculations were:

a = 9.628±0.005 Å
b = 19.256±0.010 Å
c = 6.764±0.005 Å
cos α = 0, cos β = 0, cos γ = -1/2.

would be equivalent in an hexagonal structure. This reduction of symmetry is reflected to a lesser degree in the x and y positions of all the atoms. For example, the O_{III} triangle becomes distorted from the equilateral (in accord with the change from 6_3 to 2_1) and the chlorine atom moves slightly off the screw axis.

This model for the ordering is also consistent with the observed prevalence of mimetic twinning. The tilting of neighboring PO_4 groups apparently causes the minimum energy position for the Ca_I ion to occur nearer one PO_4 group than the others [Table 3(*e*)], thus destroying the threefold symmetry of the Ca_I position. During growth or ordering of the crystal, the initial choice of Ca_I displacement direction would seem to be statistically based. Once made, this initial choice then determines all other Ca_I displacement directions, until some interruption in the ideal growth pattern, *e.g.* vacancies, would permit another initial choice to be made statistically, thus leading to mimetic twinning.

Since the ordering information can reach each column from more than one direction, the absence of one chlorine atom from one column will not block the ordering. However, it is also clear that, if enough chlorine or Ca_I ions (or both) are missing, the ordering information could become lost between filled Cl columns. Further, it is implied from the structure-refinement results that the occurrence of a chlorine vacancy tends to result in the shift of an adjacent chlorine ion past $z=\frac{1}{2}$ to the second type of site. Each such 'misplaced' chlorine atom will expand the 'wrong' oxygen triangle (Fig. 2), thus imparting to the adjacent phosphate tetrahedra a tilt that is counter to the one expected for propagation of the glide plane symmetry.

Using synthetic crystals, Prener (1967) experimented with replacing chlorine by fluorine (which then goes to $0,0,\frac{1}{4}$ in the hexagonal cell) and with driving off chlorine by heating in a vacuum. Hounslow & Chao (1970) have made observations of the dependence of monoclinic character on chlorine content in mineral chlorapatite. Both of these works suggest that 10 to 15% of the chlorine ions can be lost before the glide-plane ordering information fails to be propagated adequately and, in consequence, the hexagonal form becomes observed optically and also (Young & Elliott, 1966) with X-ray diffraction. Prener notes, however, that the splitting of the $\sim 8600^{-1}$ fluorescence line persists in the observed hexagonal form, which suggests that on a very local level the environment of the phosphate groups has symmetry lower than that imposed by the hexagonal space group $P6_3/m$. One suspects that a similar ordering might occur in hydroxyapatite; this would be a very interesting result in in view of the reported bioelectric effect on bone growth (Bassett, Pawluk & Becker, 1964).

A preliminary search for the antiferroelectric character permitted (but not required) by the glide-plane ordering of dipoles has been reported elsewhere (Elliott & Young, 1968). No antiferroelectric effect but, rather, an apparent ferroelectric effect was found. If correct, these observations must mean that the Cl ions are very easily caused to pass to their nearly equivalent positions on the opposite side of $0,\frac{1}{4},\frac{1}{2}$ ($0,0,\frac{1}{2}$, in the pseudohexagonal cell) until all (or, at least, more than one-half) of the Cl ions are on the 'same' side of the symmetry position, thus destroying the glide plane and leading to a polar space group, probably a subgroup of $P6_3$. The implied movement, for the one-half or fewer of the Cl ions that need to move, is from the center of the O'_{III} triangle containing a Cl ion in Fig. 2 to the center of the one shown without Cl, the rather small ratio ($\sim 0{\cdot}4$) of r.m.s. thermal-vibrational-amplitude to distance-to-midpoint notwithstanding. The vacancy mechanism postulated to explain occurrence of a small percentage of the Cl ions at the second sites ($z=0{\cdot}56$ and $0{\cdot}06$) could also contribute strongly to such easy shifting of Cl positions. A mechanism would thereby be provided for relatively easy motion of the boundary between antiferroelectrically ordered and ferroelectrically ordered domains and, thus, the occurrence of the ferroelectric property under action of an applied electric field (Elliott & Young, 1968) could be explained.

The authors thank Dr J. S. Prener for the specimen crystals, for many helpful discussions, and for preprints of his work. This work was supported in part by the U.S. Public Health Service through NIH-NIDR Grant DE 01912.

APPENDIX

Data collection

The X-ray intensity data were collected with an automated punched-tape-controlled single-crystal diffractometer, operating in a 2θ scan mode with unfiltered Mo $K\alpha$ radiation. A standard reflection was measured every 90 minutes. Data were collected for the reflections for which $-16 \le h \le 16$, $0 \le k \le 16$, $0 \le l \le 16$, and $25° \le 2\theta \le 100°$. The number of reflections accessible was $\sim 111{,}000$, of which 2653 were observed, 2232 were retained as valid and, of those, 2204 were crystallographically unique.

Data validation

All reflection profiles were inspected on strip-chart recorder traces. Those reflections which appeared to suffer interference from extraneous reflections were omitted from further analyses. All reflections for which positive net integrated intensity measures were obtained were treated as observed reflections (*i.e.*, no intensity measures were set to the theoretical value to be expected for an unobserved reflection), while those with negative net integrated intensity measures were deleted from any further data analyses.

Absorption correction

The single-crystal specimens were ground to spheroids and aligned with $\mathbf{c}^*$ collinear with the φ axis

of the five-circle goniostat. The reciprocal absorption factors, A^*, were taken from Table 5.3.6B of *International Tables for X-ray Crystallography* (1962). For the 0·31 mm diameter specimen μR was 0·48 and A^* ranged from 2·02 to 1·93.

Weighting scheme

The weights were σ^{-2}, where $\sigma = C_1 + C_2|F|^2$. The value used for C_1 was 0·002, while

$$C_2 = \left(\frac{1+(1+t)/S}{I_n}\right)^{1/2}$$

where I_n = net measured integrated intensity, t = ratio of the time spent in measuring the peak intensity to that spent on background, and S = signal-to-noise ratio.

References

BASSETT, C. A. L., PAWLUK, R. J. & BECKER, R. O. (1964). *Nature, Lond.* **204**, 652.

BEEVERS, C. A. & MCINTYRE, D. B. (1946). *Miner. Mag.* **27**, 254.

CROMER, D. T. (1965). *Acta Cryst.* **18**, 17.

ELLIOTT, J. C. & YOUNG, R. A. (1968). *Bull. Soc. Chim. France*, (n° Spécial), p. 1763.

HENDRICKS, S. B., JEFFERSON, M. E. & MOSLEY, V. M., (1932), *Z. Kristallogr.* **81**, 352.

HOUNSLOW, A. W. (1968). *Crystal Structure of Two Naturally Occurring Chlorapatites.* Ph. D. Thesis. Carleton Univ., Ottawa, Canada.

HOUNSLOW, A. W. & CHAO, G. Y. (1970). *Canad. Miner.* **10**, 252.

International Tables for X-ray Crystallography (1962). Vol. II, p. 302. Birmingham: Kynoch Press.

JOHNSON, C. K. (1965). *ORTEP: A Fortran Thermal-Ellipsoid Plot Program for Crystal Structure Illustrations.* Report ORNL-3794, revised. Oak Ridge National Laboratory, Oak Ridge, Tennessee.

KEPPLER, U. (1968). *Neues Jahrb. Miner. Monatsh.* p. 359.

KEPPLER, U. (1969). *Neues Jahrb. Miner. Monatsh.* p. 64.

PRENER, J. S. (1967). *J. Electrochem. Soc.* **114**, 77.

PRENER, J. S. (1971), *J. Solid State Chem.* **3**, 49.

SUDARSANAN, K. & YOUNG, R. A. (1969). *Acta Cryst.* B**25**, 1534.

SUTTON, L. E. (1958). *Interatomic Distances and Configurations in Molecules and Ions*, p. M12. London: The Chemical Society.

YOUNG, R. A. & ELLIOTT, J. C. (1966). *Arch. oral Biol.* **11**, 699.

YOUNG, R. A., & SUDARSANAN, K. & MACKIE, P. E. (1968). *Bull. Soc. Chim. France* (n° Spécial), p. 1760.

ZACHARIASEN, W. H. (1963). *Acta Cryst.* **16**, 1139.

Acta Cryst. (1972). B**28**, 1848

Structure Cristalline et Moléculaire du Bromo-1 Benzoyl-1 Phényl-2 Cyclohexane

PAR ARNAUD DUCRUIX ET CLAUDINE PASCARD-BILLY

Laboratoire de Cristallochimie, Institut de Chimie des Substances Naturelles, 91-Gif sur Yvette, France

(*Reçu le* 3 *janvier* 1972, *revu le* 21 *janvier* 1972)

1-Bromo-1-benzoyl-2-phenylcyclohexane ($C_{19}H_{19}OBr$) crystallizes in space group $P2_1/c$ with $a = 8·67$, $b = 22·13$, $c = 9·64$ Å, $\beta = 120°$ and $Z = 4$. The structure was solved by the heavy-atom technique and refined by the full-matrix least-squares method. The final R index is 0·074.

Introduction

L'étude de la déshydrohalogénation de la cétone α-bromée (I*a*) par le diéthylaminoéthanol montre que cette réaction se fait uniquement entre les atomes de brome et d'hydrogène portés respectivement par les carbones C(1) et C(6) et non entre C(1) et C(2), (Angibeaud, Rivière & Tchoubar, 1968). Le sens de la déshydrohalogénation, la réactivité de l'atome de brome, les données de la r.m.n. relatives au proton benzylique en C(2) permettent d'avancer l'hypothèse que la conformation privilégiée de (I*a*) est (I*b*).

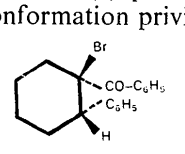

(I*a*)

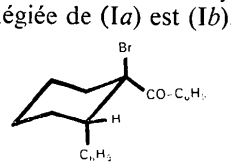

(I*b*)

Il était donc nécessaire d'obtenir confirmation directe de cette structure par la diffraction des rayons X.

Partie expérimentale

Les cristaux étudiés nous ont été fournis par M. P. Angibeaud. Les principales données expérimentales sont résumées dans le Tableau 1.

Tableau 1. *Principales données expérimentales*

Formule brute	$C_{19}H_{19}OBr$
Masse moléculaire	335
Système cristallin	monoclinique
Groupe spatial	$P2_1/c$
a	8,67 Å
b	22,136
c	9,645
β	120°
V	1603 Å^3
$F(000)$	704
Densité calculée	1,393
Densité mesurée	1,40
Nombre de réflexions indépendantes	1589
Radiation utilisée Cu $K\alpha$	1,5418 Å